



High species homology potentiates quantitative inflammation profiling in zebrafish using immunofluorescence

T. Ollewagen^{*,1}, R.M. Benecke, C. Smith

Experimental Medicine Research Group, Department of Medicine, Faculty of Medicine and Health Sciences, Stellenbosch University, South Africa

ARTICLE INFO

Keywords:

Tailfin transection
TNF- α
IL-1 β
IL-6
IL-10
MIF
MCP-1

ABSTRACT

Due to substantial homology between the human and zebrafish genome and a high level of conservation of the innate immune system across species, zebrafish larvae have become an invaluable research tool for studying inflammation and modelling inflammatory disease. However, further microscopy techniques need to be developed for better profiling of inflammation and in particular, integrated cytokine responses to different stimuli - approaches are currently largely limited to assessment of changes in cytokine gene transcription and *in vivo* visualisation using transgenics, which is limited in terms of the number of cytokines that may be assessed at once. In this study, after confirming substantial homology of human vs zebrafish cytokine amino acid sequences, immunofluorescence staining using antibodies directed at human cytokines was performed. Inflammatory cytokine signalling responses to experimental tailfin transection was assessed over 24 h (1 hpi (hours post injury), 2 hpi, 4 hpi, 24 hpi) in zebrafish larvae, with experimental end point at 120 h post fertilization (hpf). When immunofluorescence results were compared to responses observed in rodent and human literature, it is clear that the cytokines follow a similar response, albeit with a condensed total time course. Notably, tumor necrosis factor- α and monocyte chemoattractant protein-1 increased and remained elevated over the 24-h period. In contrast, interleukin-1 β and interleukin-6 peaked at 4 hpi and 2 hpi respectively but had both returned to baseline levels by 24 hpi. Macrophage migration inhibitory factor was lowest at 1 hpi, potentially encouraging macrophage movement into the site of injury, followed by a sharp increase. This protocol provides valuable insight into inflammation over a time course and more so, provides an affordable and accessible method to comprehensively assess inflammation in zebrafish disease models.

1. Introduction

Zebrafish, both adult and larval forms, have become an invaluable translational research tool and an ideal one for the modelling of human diseases specifically - especially since 2013, when their whole genome mapping was completed [1]. This demonstrated that zebrafish share 70–80 % homology with the human genome, while also having system functions similar to that of humans [2]. The innate immune system is similar in humans and zebrafish, with zebrafish macrophages present as early as 15 hours post fertilization

* Corresponding author.

E-mail address: 19687052@sun.ac.za (T. Ollewagen).

¹ Present address: Department of Medicine, Faculty of Medicine and Health Sciences, Stellenbosch University, Francie van Zijl Drive, Parow, South Africa, 7505.

<https://doi.org/10.1016/j.heliyon.2023.e23635>

Received 14 August 2023; Received in revised form 8 December 2023; Accepted 8 December 2023

Available online 13 December 2023

2405-8440/© 2023 The Authors. Published by Elsevier Ltd. This is an open access article under the CC BY-NC-ND license (<http://creativecommons.org/licenses/by-nc-nd/4.0/>).

(hpf) - phagocytosing, producing reactive oxygen species and killing pathogens by 26 hpf [3–5].

Given the many other advantages of the zebrafish model – most notably high fecundity and transparency of early larval stages – zebrafish seem the ideal model for modelling inflammation and/or inflammatory conditions. Given the central role of inflammation in disease, there is extensive literature on the use of zebrafish for the investigation of inflammation and disease modelling, highlighting the importance of zebrafish as a research tool in this context. A popular model of experimental damage - tail wounding through fin transection [5–7] - is often employed to trigger the inflammatory response for various different research purposes. However, despite the robustness of the inflammatory response and the subsequent repair and regeneration phases, application of models such as the tailfin transection model is currently limited in terms of techniques for comprehensive quantification of cytokine, chemokine and growth factor signalling.

Mapping of the zebrafish genome has resulted in pivotal research opportunities. For example, evaluation of changes in cytokine gene expression levels (which reflect gene transcription in terms of mRNA levels) of cytokines is used to quantify inflammatory signalling. The latter method has the added benefit of allowing for simultaneous assessment of multiple cytokine responses. However, given our knowledge of post-transcriptional silencing [8], gene expression may not accurately reflect events at protein level and may overestimate responses or yield false positive results.

Similarly, the creation of transgenic zebrafish whereby specific proteins fluoresce, allows for real-time *in vivo* visualisation and tracking of protein of interest – as well as cells or structures associated with them - throughout a time course or following an insult/change [9]. Although this is a powerful research tool, in the context of inflammatory signalling in particular, there are limitations to using transgenic models. Firstly, the number of proteins that can be expressed concurrently in a single transgenic line is limited and multiple individual and hybrid transgenic lines need to be developed to analyse all the required proteins/factors involved in the inflammatory pathway. Secondly, in order to create true multiple signal transgenics, the transgenic zebrafish line is required to go to the F2 generation before the larvae are considered homozygous transgenic zebrafish [10]. This process takes time, resources and specific expertise that may not be accessible in smaller laboratories. Perhaps due to these constraints, hybrid lines are often limited to two or three fluorescent proteins at most.

Furthermore, in less developed countries, and especially geographically isolated countries such as those in Southern Africa, the high cost of importation and time delays caused by customs processes regulating experimental animals, limit the feasibility of bringing existing transgenic zebrafish into the laboratories as live adults, and make it impossible to import larvae. The only remaining option is *in vitro* fertilisation of previously frozen sperm and eggs, however this efficacy is only around 50–60 % *in experienced labs* [11], which again limits the practical feasibility of this approach.

Clearly, the exploration of alternative microscopy techniques to assess cytokine responses is of extreme importance. Furthermore, the generally high homology between humans and zebrafish makes zebrafish an ideal disease modelling organism. However, the validation of such models is dependent on the capacity to confirm more comprehensively to what extent the cytokine response in zebrafish is comparable to that of humans. Therefore, using the tailfin transection model of inflammation in larval zebrafish, this study aimed to evaluate whether the transfer of immunofluorescence techniques using cytokines directed against human antigens, is a viable approach for the profiling of inflammation in zebrafish larvae.

2. Methods

2.1. Determination of human vs zebrafish cytokine homology

Sequence retrieval, alignment and homology assessment: The amino acid sequences for human and zebrafish tumor necrosis factor alpha (TNF α), tumor necrosis factor beta (TNF β), interleukin 1 beta (IL-1 β), interleukin 6 (IL-6), interleukin 10 (IL-10), macrophage migration inhibitory factor (MIF) and monocyte chemoattractant protein 1/C–C motif chemokine ligand 2 (MCP-1/CCL2) were retrieved from the UniProt and National Center for Biotechnology Information (NCBI) databases in FASTA format [12]. The obtained amino acid sequences (Supplementary Table 1) were subjected to pairwise sequence alignment using the Basic Local Alignment Search Tool (BLAST) provided by NCBI [13]. For each cytokine, the human sequence was used as the query, and the zebrafish sequence as the subject. The default parameters were used for the BLAST analysis.

Data processing and visualisation: The raw BLAST output was used to extract the percentage identities (the percentage of amino acids that match exactly between human and zebrafish cytokine amino acid sequences), percentage positives (the percentage of positions with either identical amino acids or amino acids with similar biochemical properties), and percentage gaps (the percentage of positions in the alignment with a gap in either zebrafish or human cytokine amino acid sequence). Data was compiled into a table using Python (version 3.8.10). The Python libraries pandas (version 1.2.4) and numpy (version 1.20.1) were used for data manipulation. To visualize the data, a heatmap was generated using the seaborn library (version 0.11.1) in Python. Darker colors in the heatmap represent higher percentages of identities, positives, or gaps.

2.2. Zebrafish experimental protocol

Animal husbandry & ethical considerations: All experimental protocols were approved by the Stellenbosch University Research Ethics Committee for Animal Care and Use (Ref# ACU-2021-21995). All animal experiments were carried out according to the ARRIVE guidelines and in compliance with the South African National Standard for the care and use of animals for scientific purposes. Wild-type zebrafish (*Danio rerio*) embryos were obtained from the Zebrafish Research Unit (Department Medicine, Stellenbosch University). Zebrafish embryos and larvae were maintained in embryo medium (E3; 5 mM NaCl, 0.17 mM KCl, 0.33 mM CaCl $_2$ ·2H $_2$ O, 0.33 mM

MgSO₄•7 H₂O, 1.3 × 10⁻⁵ % w/v, methylene blue in RO water) at 28.5 °C, with a 14:10 light:dark cycle.

PTU treatment: Zebrafish larvae were treated with 75 µM *N*-phenylthiourea (PTU; P7629, Sigma) in fresh embryo media daily from 4 h post fertilization (hpf) until the end of the protocol, to enhance visualisation.

Tailfin transection: Zebrafish larvae were moved to a 100 mm plastic dish and anaesthetized with 0.168 mg/ml tricaine in E3. Tailfins were transected using microscissors removing only the distal tip of the notochord. Fig. 1b and d depicts where the tailfin was cut in comparison to uncut (Fig. 1a and c). Zebrafish were placed in fresh PTU embryo media until euthanasia time points. Fish were euthanised at 1, 2, 4 and 24 hpi (hours post injury) with an overdose of tricaine (0.4 mg/ml). Tailfin transections were staggered to ensure all larval endpoints were at the same age.

Cytokine quantification: Given the high homology in amino acid sequences of inflammatory cytokines we observed, antibodies directed against human cytokines were employed to visualize the zebrafish inflammatory response to tailfin transection. Zebrafish larvae were washed in 1x phosphate buffer saline (PBS) and fixed in 4 % paraformaldehyde at 4 °C overnight. Larvae were then washed in 1x PBS +0.1 % tween-20 (PBS-T). Thereafter, larvae were placed in blocking buffer consisting of 1x PBS with 20 % foetal bovine serum (FBS), 5 % donkey serum, and 0.1 % triton-X for 3 h at room temperature. After blocking buffer was removed, primary antibodies made up in 5x diluted blocking buffer were added overnight at 4 °C. Primary antibodies included *anti*-TNF-α (1:100, NB600-587, Novus Biologicals), *anti*-IL-1β (1:200, NB600-633, Novus Biologicals), *anti*-IL-10 (1:200, ab34843, Abcam), *anti*-IL-6 (1:200, NB600-1131, Novus Biologicals), *anti*-MCP-1 (1:200, NBP1-07035, Novus Biologicals), and *anti*-MIF (1:200, ab65869, Abcam). Larvae were then washed in PBS-T prior to the addition of secondary antibody made up in 5x diluted blocking buffer at 4 °C overnight (Alexafluor 594; 1:250, A21207, Life Technologies). Larvae were washed with 1x PBS-T and finally 1x PBS before imaging. Fluorescence microscopy was performed using a Nikon ECLIPSE Ti2 inverted microscope with NIS-Elements D v5.30.02 software. Images were taken using a 10x objective, focusing on the tail region of each larva. Staining controls were utilised to optimise imaging exposure, namely an unstained control and a secondary control for AlexaFluor 594 (Supplementary Fig. 1). Primary controls were also used but showed no signal for all antibodies. While a small amount of autofluorescence is expected in zebrafish [14], the autofluorescence observed with the staining controls was minimal and localised towards the head region of the fish, and is unlikely to be a confounder in analysis of the tail. The immunofluorescent intensities were quantified within a specified area on each tailfin using colour threshold intensities on ImageJ 1.49v software (Wayne Rasband). The region of analysis was chosen to focus on the wound area and the blastema specifically, and excluded the rest of the tail region and zebrafish body – cytokines are constitutively in these areas as part of development [15–17]. A minimum of 5 samples were imaged and analysed per group.

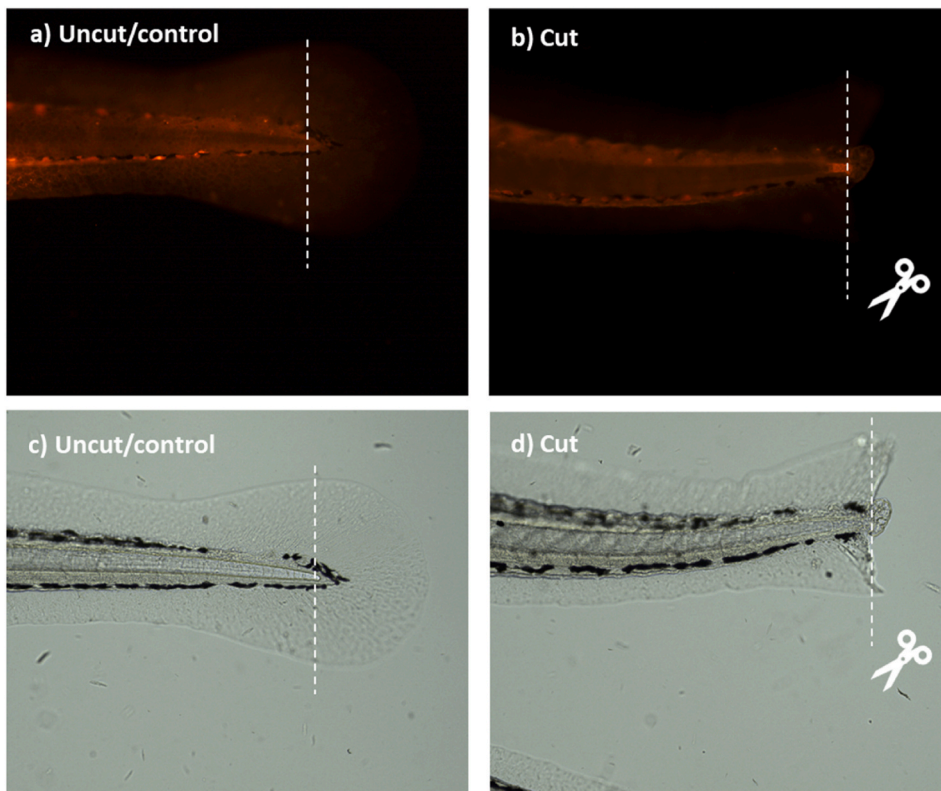


Fig. 1. Images depicting the tailfin transection method. a-b) demonstrate tailfin transection with fluorescence; c-d) depict tailfin transection with brightfield microscopy to be see the areas transected.

2.3. Statistical analysis

Statistical analysis of data were performed using GraphPad Prism v8.0.2 (<http://www.graphpad.com>, San Diego, CA). Integrated densities of each cytokine was analysed using one-way ANOVA and Tukey's multiple comparisons test. A p-value of <0.05 was considered statistically significant.

3. Results

A summary of the similarity of cytokine amino acid sequences in humans vs zebrafish is presented in Fig. 2. In general, cytokine amino acid sequences exhibited high homology across the two species. The percentage of amino acids that were exactly matched across species ranged from 22 to 69 %, but when amino acids with similar biochemical properties were also accepted, the homology increased to a range of 39–79 %, depending on the specific cytokine. Most significantly, the percentage of amino acids for which there was a gap in alignment between the species, was very low, at 0–17 %.

Cytokine labelling using fluorescently labelled anti-human cytokine antibodies, achieved good quality fluorescence signal and differential expression patterns for all cytokines, allowing comprehensive profiling of the inflammatory cytokine response to tailfin transection. When considering individual cytokine responses over time, TNF- α fluorescence was on average approximately 100 % higher at all time points after injury when compared to control. However, this increase did not reach statistical significance, likely due to a somewhat divergent response at both 4 and 24 hpi (Fig. 3a–f).

The IL-1 β response (Fig. 4a–f) seemed to have run its course over 24 hpi (ANOVA main effect of time; $p < 0.01$). Fluorescence gradually increased over the acute time points assessed but had returned to control values at 24 hpi.

IL-6 fluorescence followed a similar trajectory to that of IL-1 β , but with an even faster return to control levels (ANOVA main effect of time, $P < 0.0001$; Fig. 5a–f). IL-6 fluorescence peaked already at 2 hpi and at 4 hpi had returned to levels similar to that of uninjured controls.

Of all cytokines assessed, the results for MCP-1 were arguably the most variable (Fig. 6a–f). Nevertheless, there was an overall trend for a sustained increase in MCP-1 fluorescence following injury (ANOVA main effect of time, $P < 0.05$).

IL-10 (Fig. 7a–f) did not exhibit a significant response following tailfin transection, with fluorescence intensity remaining similar to that of uninjured controls at all time points assessed. However, at all acute time points post-injury, a small percentage of larvae exhibited large increases in IL-10 fluorescence.

In contrast to the other cytokines assessed, which all showed increased levels at early time points post-injury, MIF demonstrated and almost inverse response (ANOVA main effect of time, $P < 0.05$; Fig. 8a–f), with lowest expression at 1 hpi. At all other time points

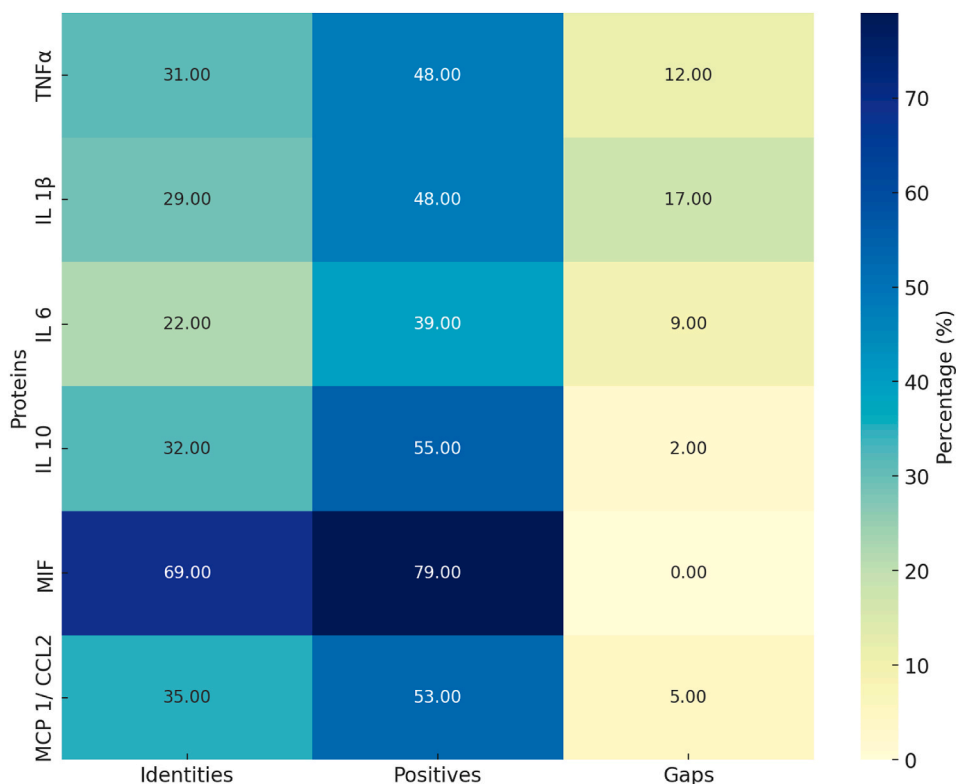


Fig. 2. Amino acid sequence alignment of human vs zebrafish cytokines. Values are expressed as percentage of total amino acids assessed.

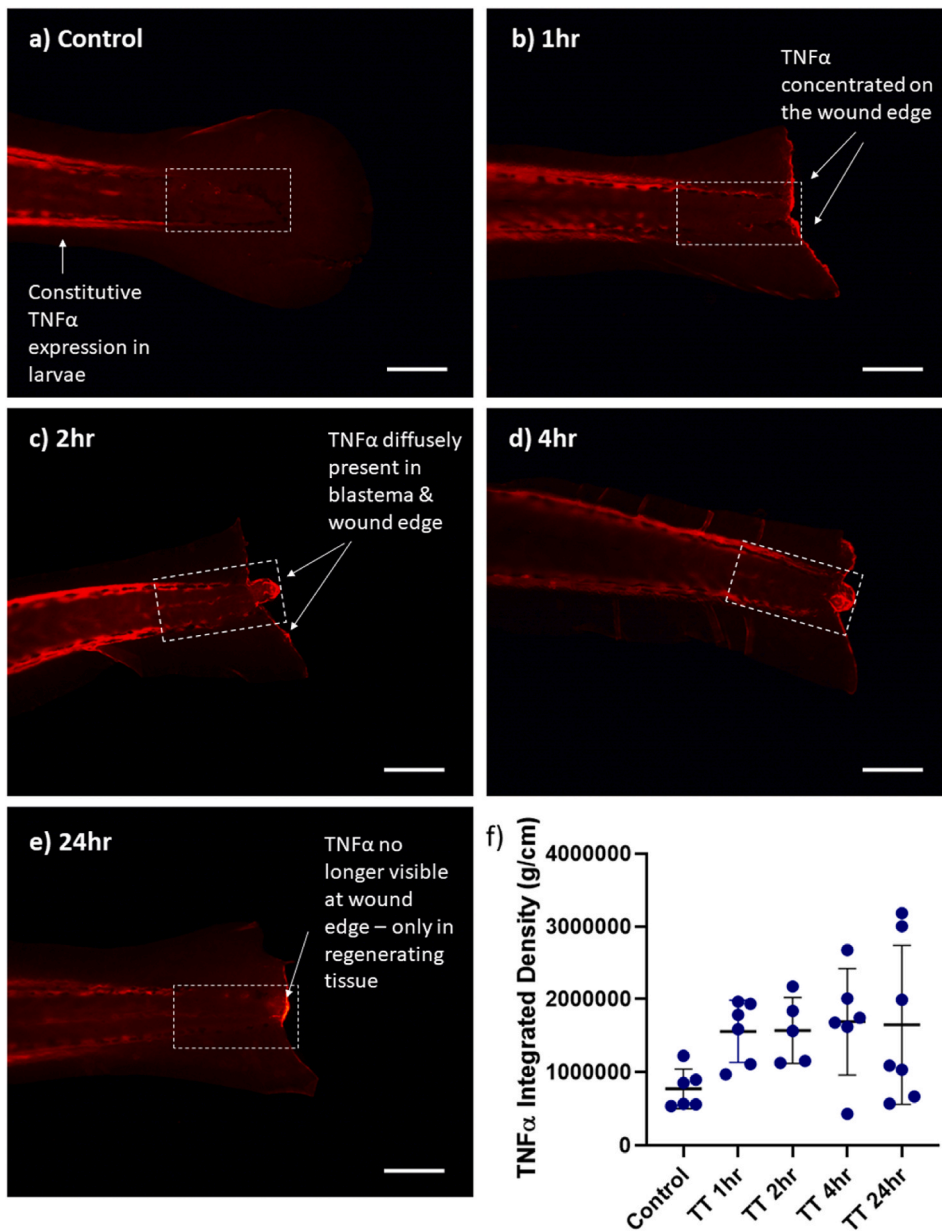


Fig. 3. Representative immunofluorescence images depicting the Tumor necrosis factor- α (TNF- α) response to tailfin transection in zebrafish larvae in a) controls, b) 1hr, c) 2hr, d) 4hr, and e) 24hr post injury. Quantified data and statistical results are presented in frame f (colour correlates to protein depiction in Fig. 9). Graph represents integrated density fluorescent intensity measurements of the defined area of the tailfin. Data are presented as mean \pm SEM. Scale bar represents 100 μ m. (For interpretation of the references to colour in this figure legend, the reader is referred to the Web version of this article.)

assessed, MIF levels were similar to that of uninjured controls.

4. Discussion

While the time frame required for inflammation and wound healing should be expected to differ between species, the cytokine response trajectories should show similar patterns, given the high level of conservation of the inflammatory immune system across species. We therefore constructed comparative cytokine response graphs (Fig. 9a–b) for zebrafish (using current data) and mammals (using published data from mammalian - human and rodent - models) to facilitate the discussion and contextualisation of current data.

Early TNF- α -expressing macrophages are vital in the development of the blastema [7,18]. Qualitatively, in the current study, following tailfin transection, the regenerative process began with the development of blastema over time. This was predominantly seen

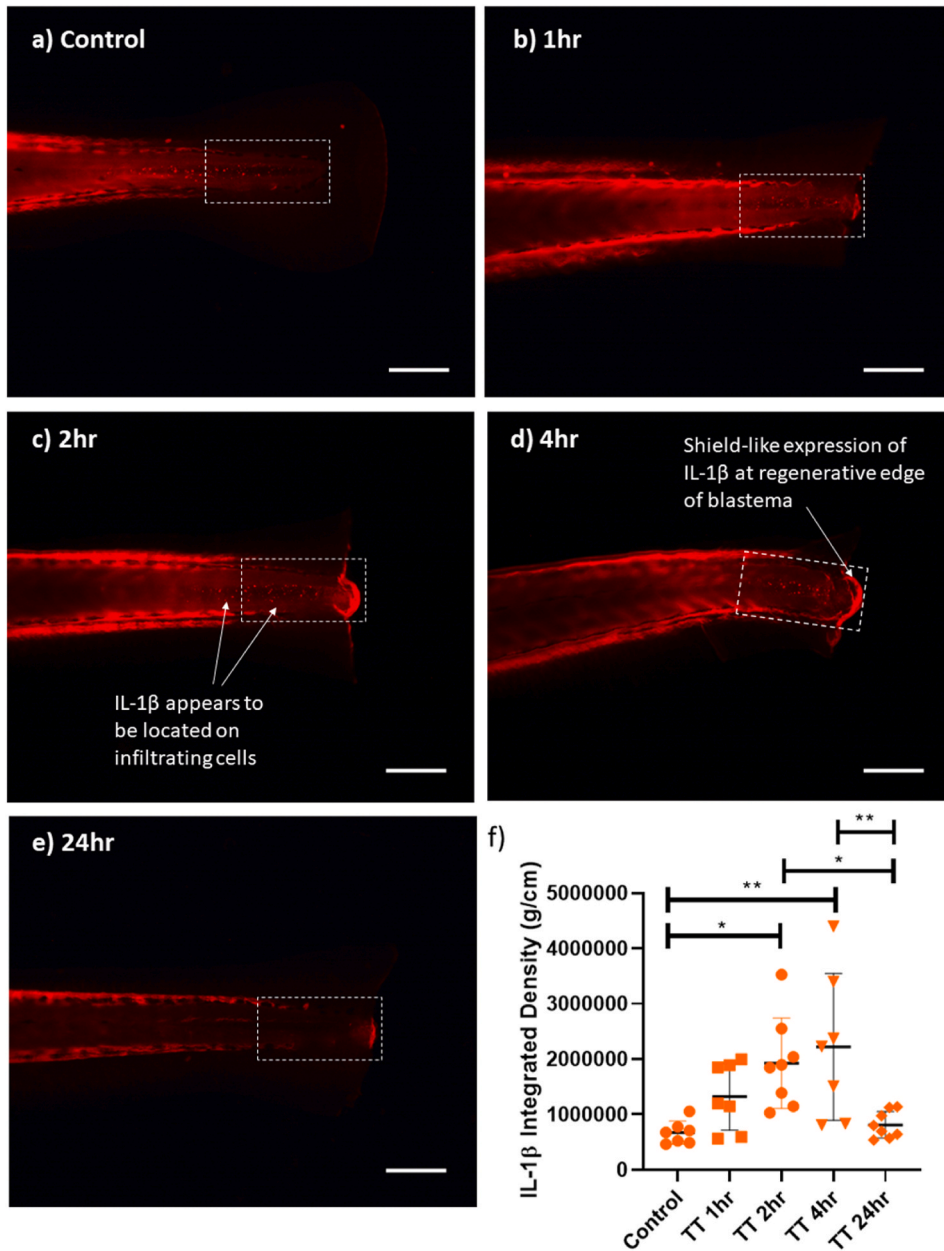


Fig. 4. Representative immunofluorescence images depicting the interleukin-1 β (IL-1 β) response to tailfin transection in zebrafish larvae in a) controls, b) 1hr, c) 2hr, d) 4hr, and e) 24hr post injury. Quantified data and statistical results are presented in frame f (colour correlates to protein depiction in Fig. 9). Graph represents integrated density fluorescent intensity measurements of the defined area of the tailfin. Data are presented as mean \pm SEM. *p < 0.05; **p < 0.01. Scale bar represents 100 μ m. (For interpretation of the references to colour in this figure legend, the reader is referred to the Web version of this article.)

at 2 and 4 hpi. Studies researching TNF- α in zebrafish largely use transgenics to investigate TNF- α alongside a macrophage marker to identify pro-inflammatory macrophages and their movement upon insult. In these studies, it was noted that macrophages arrive at the damaged site at 1 hpi, position at 6 hpi and depart around 18 hpi. These are largely TNF- α + macrophages [19,20]. With the use of an antibody directed at human TNF- α in the current study, the high species homology - which is in line with previous reports [21] - was also evident from the fact that we demonstrated a similar trend as seen in the transgenic studies discussed above. When comparing cytokine expression to that found in human studies after traumatic injury, a similar trend is noticed up to 24 hpi and then follows with a decrease over 3- and 5-days post injury (dpi) [22]. Following a traumatic brain injury in rodents, a similar trend is again demonstrated over a different time course, with TNF- α peaking around 3 hpi, remaining elevated until 8 hpi, and subsequently decreasing over the rest of the time course [23].

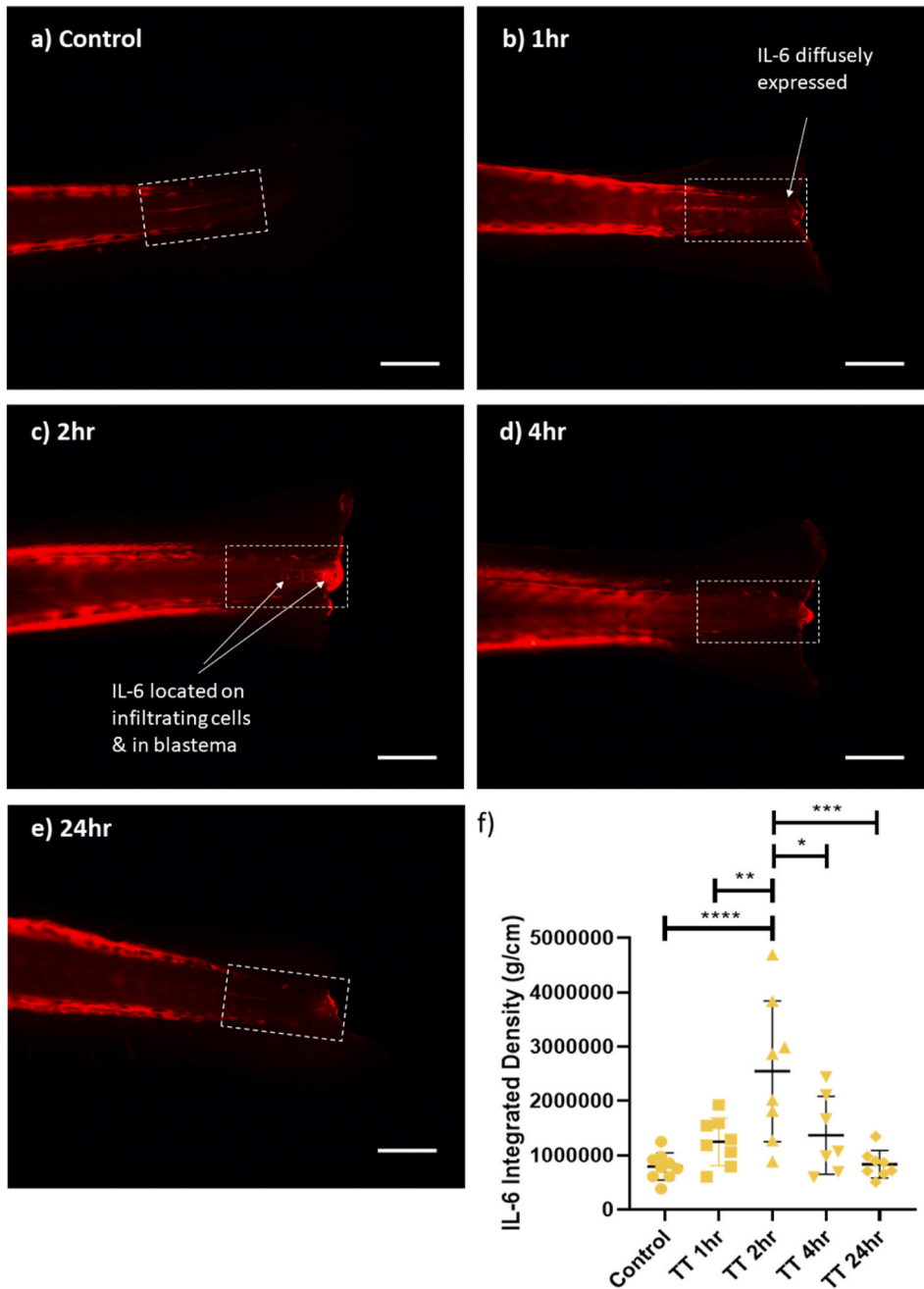


Fig. 5. Representative immunofluorescence images depicting the interleukin-6 (IL-6) response to tailfin transection in zebrafish larvae in a) controls, b) 1hr, c) 2hr, d) 4hr, and e) 24hr post injury. Quantified data and statistical results are presented in frame f (colour correlates to protein depiction in Fig. 9). Graph represents integrated density fluorescent intensity measurements of the defined area of the tailfin. Data are presented as mean ± SEM. *p < 0.05; **p < 0.01; ***p < 0.001; ****p < 0.0001. Scale bar represents 100 μm. (For interpretation of the references to colour in this figure legend, the reader is referred to the Web version of this article.)

IL-1β, another pro-inflammatory cytokine involved in the inflammatory process, is regularly assessed in tailfin transection studies. Following tailfin transection, mRNA analysis demonstrated heightened expression at 6 hpi which was reduced again at 24 hpi, more evident in panther ZF larvae [6]. In the current study, IL-1β fluorescence increased progressively at 2 and 4 hpi but returned to control levels at 24 hpi. This is in-line with another zebrafish study which also demonstrated increased levels initially followed by a sharp decrease around 12 hpi. Here they determined that IL-1β promotes regenerative factor upregulation; however, its prolonged expression resulted in apoptosis and impaired regeneration [24]. It is proposed that IL-1β acts in the early phases of regeneration followed by macrophage-derived TNF-α decreasing IL-1β to prevent early damage [6]. As discussed, a similar trend was observed with zebrafish

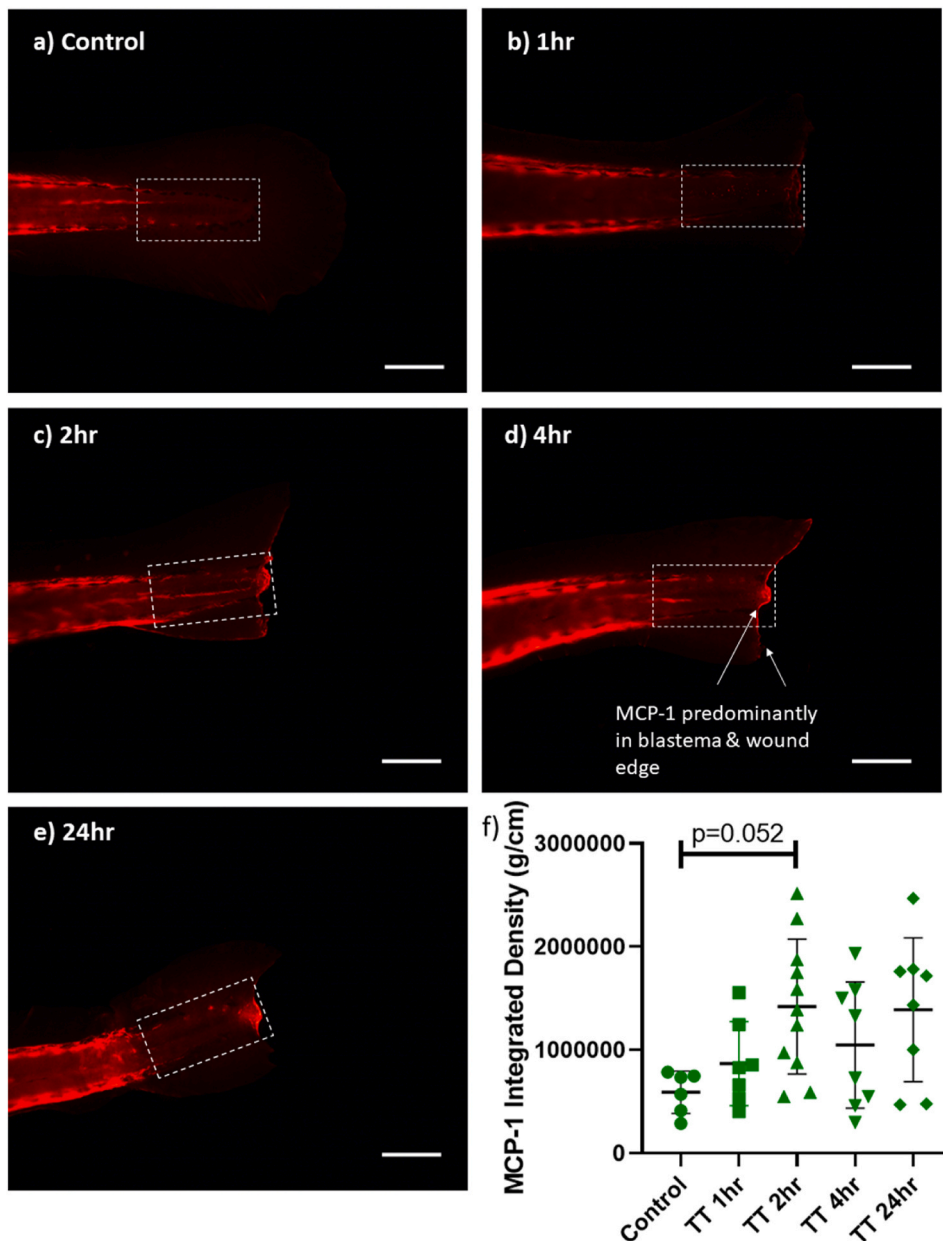


Fig. 6. Representative immunofluorescence images depicting the monocyte chemoattractant protein-1 (MCP-1) response to tailfin transection in zebrafish larvae in a) controls, b) 1hr, c) 2hr, d) 4hr, and e) 24hr post injury. Quantified data and statistical results are presented in frame f (colour correlates to protein depiction in Fig. 9). Graph represents integrated density fluorescent intensity measurements of the defined area of the tailfin. Data are presented as mean \pm SEM. Scale bar represents 100 μ m. (For interpretation of the references to colour in this figure legend, the reader is referred to the Web version of this article.)

mRNA or in situ hybridization analysis and the current protein-based fluorescence, demonstrating a positive outcome using human antibodies for detection in zebrafish. This may be due to genetic similarities with zebrafish IL-1 β sharing a β -sheet-rich trefoil structure with the human IL-1 β [25]. When compared to a rodent model of nerve regeneration, IL-1 β followed the same trend but over a longer period of time, with the peak values demonstrated at 3 dpi [26]. This differs based on severity of the injury but continues to demonstrate a similar curve over time [27] as illustrated in zebrafish (Fig. 9a–b). In another rodent brain injury study, IL-1 peaks around 8 hpi and subsequently decreases [23], also demonstrating this similar trend. This insult-dependence of time course further highlights the need for the approach we suggest here, as this would allow more comprehensive assessments over time in various models.

While IL-6 expression over time has not been discussed in terms of tailfin transection, it has been demonstrated to have protective

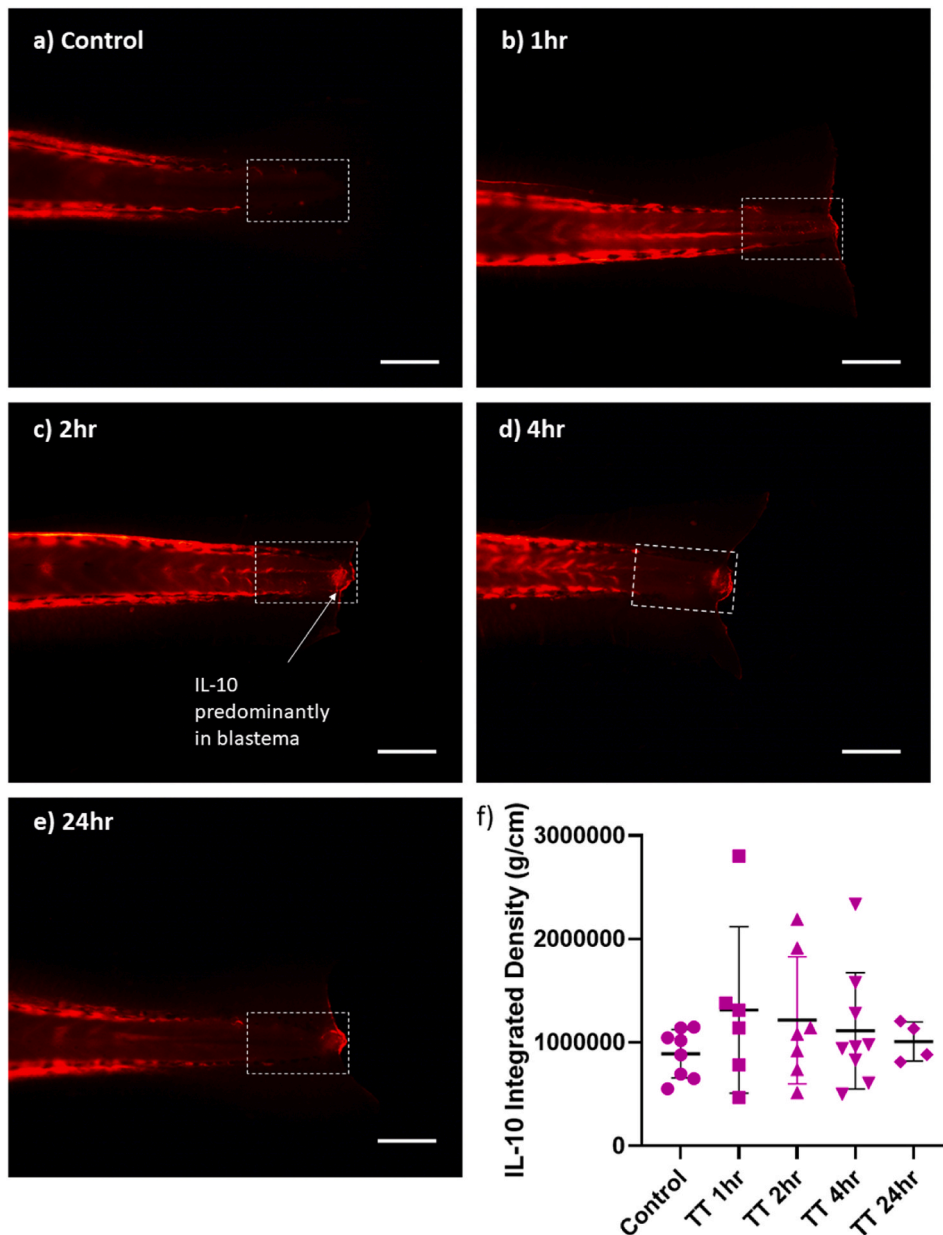


Fig. 7. Representative immunofluorescence images depicting the interleukin-10 (IL-10) response to tailfin transection in zebrafish larvae in a) controls, b) 1hr, c) 2hr, d) 4hr, and e) 24hr post injury. Quantified data and statistical results are presented in frame f (colour correlates to protein depiction in Fig. 9). Graph represents integrated density fluorescent intensity measurements of the defined area of the tailfin. Data are presented as mean \pm SEM. Scale bar represents 100 μ m. (For interpretation of the references to colour in this figure legend, the reader is referred to the Web version of this article.)

effects upon larval exposure to *Staphylococcus epidermidis*. Under infection conditions, its increase is slightly delayed compared to that of $\text{TNF-}\alpha$ and $\text{IL-1}\beta$ [28], which is somewhat different to that found following tailfin transection in the current study. Here, IL-6 peaked at 2 hpi. It did, however, follow a similar trend as $\text{IL-1}\beta$ fluorescence with the return to control levels at 24 hpi. This decrease was similar to that observed 24 h after exposure to LPS [17]. This may demonstrate a similar protective role as $\text{IL-1}\beta$ in tissue regeneration. Importantly, in addition to the high homology in amino acid sequence reported in the current study, zebrafish IL-6 presents a high structural similarity to human IL-6 [17] supporting the feasibility of using an anti-human IL-6 antibody in zebrafish. Furthermore, when comparing time course and trends to rodent or human studies (Fig. 9b), IL-6 followed the same trend over a longer period of time as the zebrafish IL-6 (Fig. 9a) following traumatic brain injury in rodents, with IL-6 peaking at 8 hpi and decreasing to control levels at 72 hpi [23]. The same peak and time course was observed with a closed head injury in rats [29].

The CCL2 (MCP-1)/CCR2 axis is known to contribute to inflammation following both exposure to infection and to tailfin

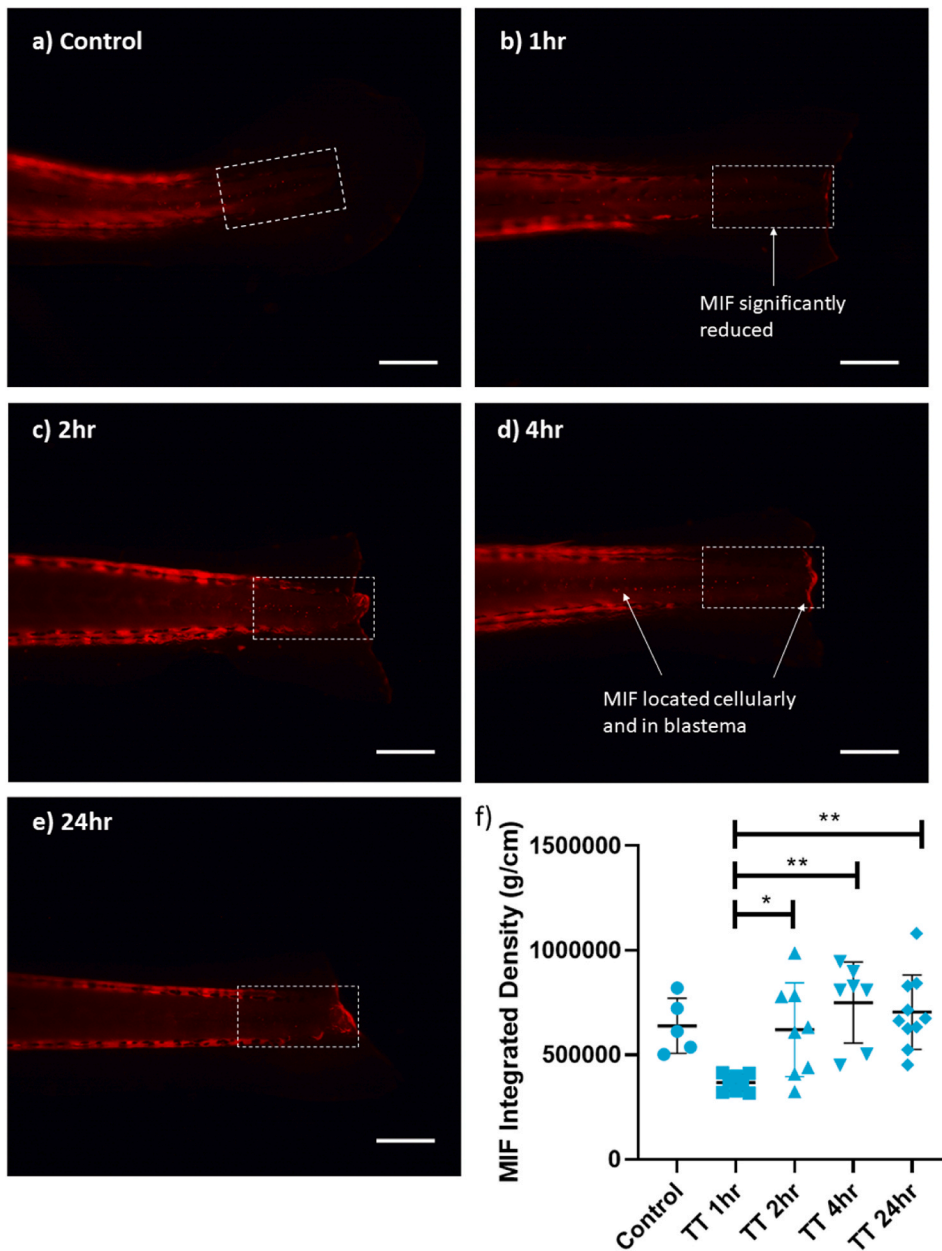


Fig. 8. Representative immunofluorescence images depicting the macrophage migration inhibitory factor (MIF) response to tailfin transection in zebrafish larvae in a) controls, b) 1hr, c) 2hr, d) 4hr, and e) 24hr post injury. Quantified data and statistical results are presented in frame f (colour correlates to protein depiction in Fig. 9). Graph represents integrated density fluorescent intensity measurements of the defined area of the tailfin. Data are presented as mean \pm SEM. * $p < 0.05$; ** $p < 0.01$. Scale bar represents 100 μ m. (For interpretation of the references to colour in this figure legend, the reader is referred to the Web version of this article.)

transection; however, this response has not been quantified over time – this is another novel aspect of the current study. Furthermore, injection of human CCL2 into the hindbrain of zebrafish embryos efficiently recruited macrophages to the area when compared to a PBS control [30], again showing the potential homology in human vs zebrafish cytokines. Despite the importance of MCP-1 in macrophage recruitment and therefore in wound healing, further research in this regard is limited in zebrafish. In the current study, MCP-1 showed a trend for elevation following injury, but high variability in individual responses was observed. This variability may be due to actual inter-individual variability in cytokine response, but this is unlikely, given the relatively more uniform responses seen for other cytokines. A more likely explanation could be that slight differences in the extent of transection-induced damage resulted in this variation. The somewhat divergent profile seen for $TNF-\alpha$ - suggesting earlier return to normal in larvae with relatively less damage, while more damage resulted in a sustained elevation of cytokine levels - supports this notion. When comparing trends to rodent and

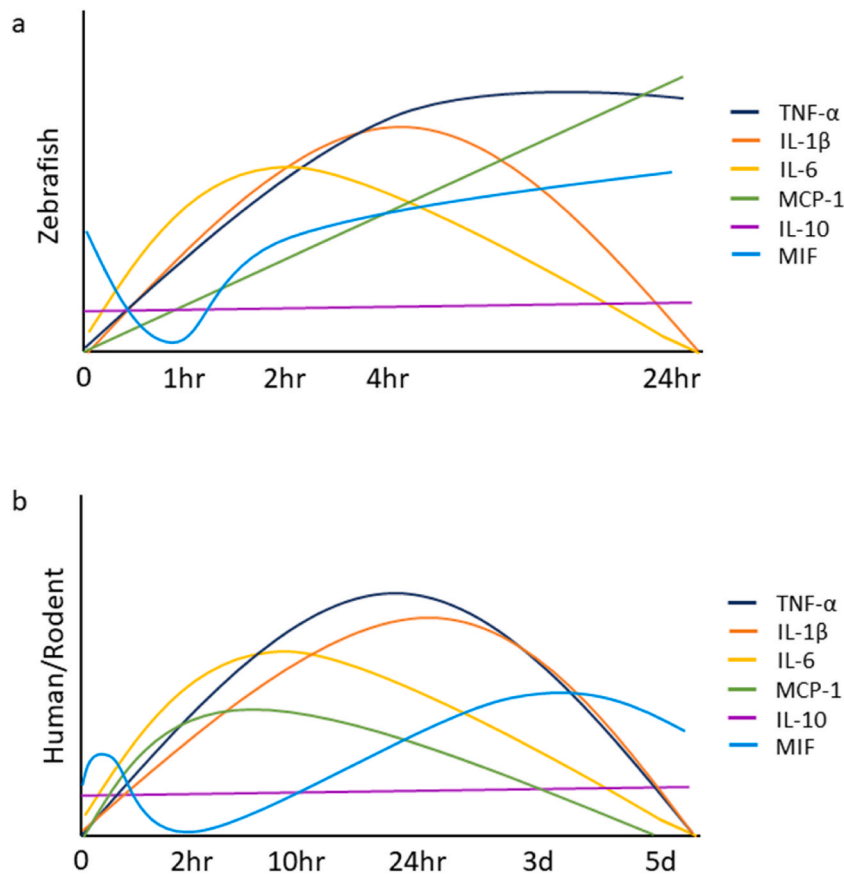


Fig. 9. Representative graphs comparing the (a) zebrafish immunofluorescent staining results with (b) general and predicted trends observed for cytokine responses to acute injury in human and rodent models as described in the text below.

human studies (Fig. 9b), cryogenic lesion in a rodent brain resulted in MCP-1 peaking at 6 h post injury. This was maintained at 24 h and started to decline at 48 h post injury [31]. In human traumatic brain injury, MCP-1 remained elevated until after day 2 showing similar increases as observed in the current study. However, in the same study using mice traumatic brain injury, MCP-1 peaked at 4 h post injury and was maintained until a slight decrease at 24 h [32].

LPS induces an inflammatory response with the increase in both pro- and anti-inflammatory cytokines, including IL-10 [33]. RNA analysis in zebrafish demonstrates a similar trend to IL-1β with a sharp increase at 2 hpi and a return to control levels at 24 hpi [34]. However, in the current study, IL-10 did not differ significantly at any time point when compared to the uninjured control. However, if we consider the variability seen between 1 and 4 hpi and the return to similarity at 24 hpi, we can see that there is a level of responsiveness in the different zebrafish. While IL-10-deficient zebrafish introduced to an inflammatory insult do not demonstrate altered inflammatory response in the early stages, it does significantly increase the pro-inflammatory status in the later stages (ie after 8 h) [35,36], highlighting its important immunomodulatory role. When compared to rodents, following sciatic nerve crush injury, IL-10 mRNA was only increased after 7 days [37]. It is possible that the time points measured in the zebrafish are not sufficient to show this spike. However, in the zebrafish model, there were certain samples that were considerably higher than the rest at the time point. This may indicate severity of damage that increases the IL-10 at an early stage to manage the inflammatory response. It is also possible that there are sustained levels of IL-10 in the zebrafish contributing to repair and regeneration as seen with spinal cord injuries [38].

MIF contributes to the inhibition of random macrophage migration. Furthermore, in zebrafish, MIF is vital for normal embryonic development [39]. In this study, the lowest fluorescence expression of MIF was observed at 1 hpi, lower than that of the control larvae, followed by a significant increase at 2, 4 and 24 hpi. This indicates a reduction in the inhibition of macrophages to the site of injury, thereafter increasing the inhibition to facilitate regeneration. Further contributing to its protective role, in a rodent model, IL-1β increases the expression of MIF [40], reducing macrophage infiltration, thereby reducing IL-1β and preventing early damage induced by excessive IL-1β [6]. Based on the trends of the cytokines observed, this protective effect may happen within the 24-h period. Genetically, the zebrafish coding sequence predicts a 115 amino acid protein - the same as the mammalian MIF - with a predicted 69% similarity [41] further validating current data. Furthermore, MIF expression in rat skin after excision demonstrated a biphasic response (Fig. 9), with a peak expression demonstrated at 3 and again at 24 hpi, with a transient decrease at 6 hpi [42]. In contrast, after spinal cord injury, which is arguably a more severe insult, MIF was reported to peak at 4 dpi [43]. However, since the first assessment was only performed at 1 dpi, a biphasic curve may have been missed. Alternatively, nerve involvement may have added complexity to the

response. The current study may also have missed this biphasic curve with the 1-h timepoint clearly demonstrating a sharp decrease. Given the relatively short time-trajectories for cytokine responses in zebrafish, it is likely that a first peak may have been missed with the current sampling time protocol. Inclusion of more time points will shed more light on this.

In summary, contextualisation of current data on inflammatory cytokine time courses consistently corresponds with those reported in literature. This suggests that current data indeed provide evidence of the feasibility of mapping the inflammatory response in zebrafish using anti-human antibodies. The current approach allows for expansion on current literature by providing a more integrated signalling profile incorporating multiple cytokines over time. In terms of potential limitations, the anti-human antibodies used for immunofluorescence were not validated using zebrafish-specific reagents, as these were not available to us. Laboratories with more resources could potentially contribute to confirmation of these techniques that are more feasible to lower resource settings. For example, a Western blot validation method was previously demonstrated, where CRISPR/Cas9 knockdown of the zebrafish *tnf- α* gene was confirmed with the use of an anti-zebrafish TNF- α antibody to illustrate the resulting reduced protein levels [44]. However, consideration needs to be made as zebrafish often express multiple paralogues of similar sequence and size, reducing the feasibility of size-based identification [45]. Similarly, the use of cytokine knockdown fish is also limited by the paralogue's phenomenon – identification of and knocking down all associated paralogues would be near impossible. Alternatively, parallel assessment of cytokine responses using antibodies directed against anti-human cytokines vs transgenic zebrafish with fluorescent gene reporters may confirm similarity of data generated. We do acknowledge that further investigation into the validation of anti-human antibody use in zebrafish is required. Thus, until such time when these methods have been proven to yield reproducible results across research laboratories and in line with data achieved by best-practise methodology, interpretation of data should err on the side of caution. In particular, researchers in low resource settings opting for the use of immunofluorescent labelling, are reminded to consider the possibility of nonspecific binding of antibodies. We recommend that they take care to research the predicted binding sites of antibodies and whether it corresponds with literature using transgenic reporters or staining in other models. Nevertheless, the current data on amino acid sequence homology and the similarity in the zebrafish cytokine responses over time when compared to those reported in mammals, validates our approach – it is highly unlikely that non-specific binding will result in responses almost exactly mimicking those in mammals for every cytokine assessed.

In conclusion, the immunofluorescence approach for quantitation presented here, potentially provides an accessible and affordable technique requiring only standard wildtype zebrafish, which enables cytokine profiling which is applicable to both zebrafish and human research applications in the inflammation and regeneration niche.

Ethics declarations

This study was reviewed and approved by Stellenbosch University Research Ethics Committee for Animal Care and Use, with the approval number: ACU-2021-21995). All animal experiments were carried out according to the ARRIVE guidelines and in compliance with the South African National Standard for the care and use of animals for scientific purposes.

Funding

This work was supported by the South African National Research Foundation (SRUG2203301243 and PDG210406592305). We would also like to acknowledge kind donations from Prof Jean Millar and Prof Robert Fenn, which contributed towards maintenance of the zebrafish facility and staff salaries.

Data availability statement

All data is presented in the manuscript and supplementary files. Raw image data will be made available on request.

CRediT authorship contribution statement

T. Ollewagen: Writing – review & editing, Writing – original draft, Visualization, Validation, Project administration, Methodology, Investigation, Formal analysis, Data curation, Conceptualization. **R.M. Benecke:** Software, Formal analysis, Data curation. **C. Smith:** Writing – review & editing, Supervision, Resources, Project administration, Funding acquisition, Formal analysis, Conceptualization.

Declaration of competing interest

The authors declare the following financial interests/personal relationships which may be considered as potential competing interests: Tracey Ollewagen reports financial support was provided by National Research Fund South Africa.

Appendix A. Supplementary data

Supplementary data to this article can be found online at <https://doi.org/10.1016/j.heliyon.2023.e23635>.

References

- [1] K. Howe, M.D. Clark, C.F. Torroja, J. Torrance, C. Berthelot, M. Muffato, J.E. Collins, S. Humphray, K. McLaren, L. Matthews, S. McLaren, I. Sealy, M. Caccamo, C. Churcher, C. Scott, J.C. Barrett, R. Koch, G.J. Rauch, S. White, W. Chow, B. Kilian, L.T. Quintais, J.A. Guerra-Assunção, Y. Zhou, Y. Gu, J. Yen, J.H. Vogel, T. Eyre, S. Redmond, R. Banerjee, J. Chi, B. Fu, E. Langley, S.F. Maguire, G.K. Laird, D. Lloyd, E. Kenyon, S. Donaldson, H. Sehra, J. Almeida-King, J. Loveland, S. Trevanion, M. Jones, M. Quail, D. Willey, A. Hunt, J. Burton, S. Sims, K. McIlroy, B. Plumb, J. Davis, C. Clee, K. Oliver, R. Clark, C. Riddle, D. Elliott, G. Threadgold, G. Harden, D. Ware, B. Mortimer, G. Kerry, P. Heath, B. Phillimore, A. Tracey, N. Corby, M. Dunn, C. Johnson, J. Wood, S. Clark, S. Pelan, G. Griffiths, M. Smith, R. Glithero, P. Howden, N. Barker, C. Stevens, J. Harley, K. Holt, G. Panagiotidis, J. Lovell, H. Beasley, C. Henderson, D. Gordon, K. Auger, D. Wright, J. Collins, C. Raisen, L. Dyer, K. Leung, L. Robertson, K. Ambridge, D. Leongamornlert, S. McGuire, R. Gilderthorpe, C. Griffiths, D. Manthavadi, S. Nichol, G. Barker, S. Whitehead, M. Kay, J. Brown, C. Murnane, E. Gray, M. Humphries, N. Sycamore, D. Barker, D. Saunders, J. Wallis, A. Babbage, S. Hammond, M. Mashreghy-Mohammadi, L. Barr, S. Martin, P. Wray, A. Ellington, N. Matthews, M. Ellwood, R. Woodmansey, G. Clark, J. Cooper, A. Tromans, D. Grahham, C. Skuce, R. Pandian, R. Andrews, E. Harrison, A. Kimberley, J. Garnett, N. Fosker, R. Hall, P. Garner, D. Kelly, C. Bird, S. Palmer, I. Gehring, A. Berger, C.M. Dooley, J. Ersan-Urün, C. Eser, H. Geiger, M. Geisler, L. Karotki, A. Kirn, J. Konantz, M. Konantz, M. Oberländer, S. Rudolph-Geiger, M. Teucke, K. Osoegawa, B. Zhu, A. Rapp, S. Widaa, C. Langford, F. Yang, N.P. Carter, J. Harrow, Z. Ning, J. Herrero, S.M.J. Searle, A. Enright, R. Geisler, R.H.A. Plasterk, C. Lee, M. Westerfield, P.J. De Jong, L.I. Zon, J.H. Postlethwait, C. Nüsslein-Volhard, T.J.P. Hubbard, H.R. Crollius, J. Rogers, D.L. Stemple, The zebrafish reference genome sequence and its relationship to the human genome, *Nature* 496 (2013) 498–503, <https://doi.org/10.1038/nature12111>.
- [2] J.B. Phillips, M. Westerfield, Zebrafish models in translational research: tipping the scales toward advancements in human health, *DMM Dis. Model. Mech.* 7 (2014) 739–743, <https://doi.org/10.1242/dmm.015545>.
- [3] P. Herbomel, B. Thisse, C. Thisse, Ontogeny and behaviour of early macrophages in the zebrafish embryo, *Development* 126 (1999) 3735–3745, [https://doi.org/10.1016/S0960-9822\(99\)80407-2](https://doi.org/10.1016/S0960-9822(99)80407-2).
- [4] A.C. Hermann, P.J. Millard, S.L. Blake, C.H. Kim, Development of a respiratory burst assay using zebrafish kidneys and embryos, *J. Immunol. Methods* 292 (2004) 119–129, <https://doi.org/10.1016/j.jim.2004.06.016>.
- [5] Y. Xie, A.H. Meijer, M.J.M. Schaaf, Modeling inflammation in zebrafish for the development of anti-inflammatory drugs, *Front. Cell Dev. Biol.* 8 (2021), <https://doi.org/10.3389/fcell.2020.620984>.
- [6] R.A. Morales, M.L. Allende, Peripheral macrophages promote tissue regeneration in zebrafish by fine-tuning the inflammatory response, *Front. Immunol.* 10 (2019) 1–14, <https://doi.org/10.3389/fimmu.2019.00253>.
- [7] C. Bohaud, M.D. Johansen, C. Jorgensen, N. Ipeizl, L. Kremer, F. Djouad, The role of macrophages during zebrafish injury and tissue regeneration under infectious and non-infectious conditions, *Front. Immunol.* 12 (2021) 1–9, <https://doi.org/10.3389/fimmu.2021.707824>.
- [8] I.V. St Louis, P.R. Bohjanen, Post-transcriptional regulation of cytokine and growth factor signaling in cancer, *Cytokine Growth Factor Rev.* 33 (2017) 83–93, <https://doi.org/10.4049/jimmunol.1801473>.
- [9] C.P. Choe, S.-Y. Choi, Y. Kee, M.J. Kim, S.-H. Kim, Y. Lee, H.-C. Park, H. Ro, Transgenic fluorescent zebrafish lines that have revolutionized biomedical research, *Lab. Anim. Res.* 37 (2021) 1–29, <https://doi.org/10.1186/s42826-021-00103-2>.
- [10] S. Berghmans, C. Jette, D. Langenau, K. Hsu, R. Stewart, T. Look, J.P. Kanki, Making waves in cancer research: new models in the zebrafish, *Biotechniques* 39 (2005) 227–237, <https://doi.org/10.2144/05392RV02>.
- [11] Z. Marinović, Q. Li, J. Lujčić, Y. Iwasaki, Z. Csenki, B. Urbányi, G. Yoshizaki, Á. Horváth, Preservation of zebrafish genetic resources through testis cryopreservation and spermatogonia transplantation, *Sci. Rep.* 9 (2019) 1–10, <https://doi.org/10.1038/s41598-019-50169-1>.
- [12] E.W. Sayers, E.E. Bolton, J.R. Brister, K. Canese, J. Chan, D.C. Comeau, C.M. Farrell, M. Feldgarden, A.M. Fine, K. Funk, E. Hatcher, S. Kannan, C. Kelly, S. Kim, W. Klimke, M.J. Landrum, S. Lathrop, Z. Lu, T.L. Madden, A. Malheiro, A. Marchler-Bauer, T.D. Murphy, L. Phan, S. Pujar, S.H. Rangwala, V.A. Schneider, T. Tse, J. Wang, J. Ye, B.W. Trawick, K.D. Pruitt, S.T. Sherry, Database resources of the national center for Biotechnology information in 2023, *Nucleic Acids Res.* 51 (2023) D29–D38, <https://doi.org/10.1093/nar/gkac1032>.
- [13] S.F. Altschul, W. Gish, W. Miller, E.W. Myers, D.J. Lipman, Basic local alignment search tool, *J. Mol. Biol.* 215 (1990) 403–410, [https://doi.org/10.1016/S0022-2836\(05\)80360-2](https://doi.org/10.1016/S0022-2836(05)80360-2).
- [14] H. Hogset, C.C. Horgan, J.P.K. Armstrong, M.S. Bergholt, V. Torraca, Q. Chen, T.J. Keane, L. Bugeon, M.J. Dallman, S. Mostowy, M.M. Stevens, In vivo biomolecular imaging of zebrafish embryos using confocal Raman spectroscopy, *Nat. Commun.* 11 (2020) 1–12, <https://doi.org/10.1038/s41467-020-19827-1>.
- [15] K. Ito, F. Takizawa, Y. Yoshiura, M. Ototake, T. Nakanishi, Expression profile of cytokine and transcription factor genes during embryonic development of zebrafish *Danio rerio*, *Fish. Sci.* 74 (2008) 391–396, <https://doi.org/10.1111/j.1444-2906.2008.01526.x>.
- [16] M. Van Der Vaart, O. Svoboda, B.G. Weijts, R. Espín-Palazón, V. Sapp, T. Pietri, M. Bagnat, A.R. Muotri, D. Traver, *Mecp2* regulates *tnfa* during zebrafish embryonic development and acute inflammation, *DMM Dis. Model. Mech.* 10 (2017) 1439–1451, <https://doi.org/10.1242/dmm.026922>.
- [17] M. Varela, S. Dios, B. Novoa, A. Figueras, Characterisation, expression and ontogeny of interleukin-6 and its receptors in zebrafish (*Danio rerio*), *Dev. Comp. Immunol.* 37 (2012) 97–106, <https://doi.org/10.1016/j.dci.2011.11.004>.
- [18] M. Nguyen-Chi, B. Laplace-Builhé, J. Travnickova, P. Luz-Crawford, G. Tejedor, G. Lutfalla, K. Kissa, C. Jorgensen, F. Djouad, TNF signaling and macrophages govern fin regeneration in zebrafish larvae, *Cell Death Dis.* 8 (2017), <https://doi.org/10.1038/CDDIS.2017.374>.
- [19] C. Bohaud, M.D. Johansen, B. Varga, R. Contreras-Lopez, A. Barthelaix, C. Hamela, D. Sapède, T. Cloitre, C. Gergely, C. Jorgensen, L. Kremer, F. Djouad, Exploring macrophage-dependent wound regeneration during mycobacterial infection in zebrafish, *Front. Immunol.* 13 (2022) 1–16, <https://doi.org/10.3389/fimmu.2022.838425>.
- [20] M. Nguyen-Chi, B. Laplace-Builhé, J. Travnickova, P. Luz-Crawford, G. Tejedor, Q.T. Phan, I. Duroux-Richard, J.P. Levraud, K. Kissa, G. Lutfalla, C. Jorgensen, F. Djouad, Identification of polarized macrophage subsets in zebrafish, *Elife* 4 (2015) 1–14, <https://doi.org/10.7554/eLife.07288>.
- [21] Y. Duan, Y. Wang, Z. Li, L. Ma, X. Wei, J. Yang, R. Xiao, C. Xia, The unique structure of the zebrafish TNF- α homotrimer, *Dev. Comp. Immunol.* 122 (2021), 104129, <https://doi.org/10.1016/j.dci.2021.104129>.
- [22] C. Liu, J. Tang, Expression levels of tumor necrosis factor- α and the corresponding receptors are correlated with trauma severity, *Oncol. Lett.* 8 (2014) 2747–2751, <https://doi.org/10.3892/ol.2014.2575>.
- [23] V. Taupin, S. Toulmond, A. Serrano, J. Benavides, F. Zavala, Increase in IL-6, IL-1 and TNF levels in rat brain following traumatic lesion. Influence of pre- and post-traumatic treatment with Ro5 4864, a peripheral-type (p site) benzodiazepine ligand, *J. Neuroimmunol.* 42 (1993) 177–185, [https://doi.org/10.1016/0165-5728\(93\)90008-M](https://doi.org/10.1016/0165-5728(93)90008-M).
- [24] T. Hasegawa, C.J. Hall, P.S. Crosier, G. Abe, K. Kawakami, A. Kudo, A. Kawakami, Transient inflammatory response mediated by interleukin-1 β is required for proper regeneration in zebrafish fin fold, *Elife* 6 (2017) 1–22, <https://doi.org/10.7554/eLife.22716>.
- [25] N.V. Ogryzko, E.E. Hoggett, S. Solaymani-Kohal, S. Tazzyman, T.J.A. Chico, S.A. Renshaw, H.L. Wilson, Zebrafish tissue injury causes upregulation of interleukin-1 and caspase-dependent amplification of the inflammatory response, *DMM Dis. Model. Mech.* 7 (2014) 259–264, <https://doi.org/10.1242/dmm.013029>.
- [26] R. Wu, B. Chen, X. Jia, Y. Qiu, M. Liu, C. Huang, J. Feng, Q. Wu, Interleukin-1 β influences functional regeneration following nerve injury in mice through nuclear factor- κ B signaling pathway, *Immunology* 156 (2019) 235–248, <https://doi.org/10.1111/imm.13022>.
- [27] T. Woodcock, M.C. Morganti-Kossmann, The role of markers of inflammation in traumatic brain injury, *Front. Neurol.* 4 (2013) 1–18, <https://doi.org/10.3389/fneur.2013.00018>.
- [28] P.T. Dhanagovind, P.K. Kujur, R.K. Swain, S. Banerjee, IL-6 signaling protects zebrafish larvae during *Staphylococcus epidermidis* infection in a bath immersion model, *J. Immunol.* 207 (2021) 2129–2142, <https://doi.org/10.4049/jimmunol.2000714>.
- [29] E. Shohami, M. Novikov, R. Bass, A. Yamin, R. Gallily, Closed head injury triggers early production of TNF α and IL-6 by brain tissue, *J. Cerebr. Blood Flow Metabol.* 14 (1994) 615–619, <https://doi.org/10.1038/jcbfm.1994.76>.
- [30] F. Sommer, N.V. Ortiz Zacarias, L.H. Heitman, A.H. Meijer, Inhibition of macrophage migration in zebrafish larvae demonstrates in vivo efficacy of human CCR2 inhibitors, *Dev. Comp. Immunol.* 116 (2021), <https://doi.org/10.1016/j.dci.2020.103932>.

- [31] D. Grzybicki, S.A. Moore, R. Schelper, A.R. Glabinski, R.M. Ransohoff, S. Murphy, Expression of monocyte chemoattractant protein (MCP-1) and nitric oxide synthase-2 following cerebral trauma, *Acta Neuropathol.* 95 (1997) 98–103, <https://doi.org/10.1007/s004010050770>.
- [32] B.D. Semple, N. Bye, M. Rancan, J.M. Ziebell, M.C. Morganti-Kossmann, Role of CCL2 (MCP-1) in traumatic brain injury (TBI): evidence from severe TBI patients and CCL2-/- mice, *J. Cerebr. Blood Flow Metabol.* 30 (2010) 769–782, <https://doi.org/10.1038/jcbfm.2009.262>.
- [33] A.M. Phillip, Y. Wang, A. Mauro, S. El-Rass, J.C. Marshall, W.L. Lee, A.S. Slutsky, C.C. dos Santos, X.Y. Wen, Development of a zebrafish sepsis model for high-throughput drug discovery, *Mol. Med.* 23 (2017) 134–148, <https://doi.org/10.2119/molmed.2016.00188>.
- [34] L. Li, B. Yan, Y.Q. Shi, W.Q. Zhang, Z.L. Wen, Live imaging reveals differing roles of macrophages and neutrophils during zebrafish tail fin regeneration, *J. Biol. Chem.* 287 (2012) 25353–25360, <https://doi.org/10.1074/jbc.M112.349126>.
- [35] F. Bottiglione, C.T. Dee, R. Lea, L.A.H. Zeef, A.P. Badrock, M. Wane, L. Bugeon, M.J. Dallman, J.E. Allen, A.F.L. Hurlstone, Zebrafish IL-4-like cytokines and IL-10 suppress inflammation but only IL-10 is essential for gill homeostasis, *J. Immunol.* 205 (2020) 994–1008, <https://doi.org/10.4049/jimmunol.2000372>.
- [36] R.A. Morales, S. Rabahi, O.E. Diaz, Y. Salloum, B.C. Kern, M. Westling, X. Luo, S.M. Parigi, G. Monasterio, S. Das, P.P. Hernández, E.J. Villablanca, Interleukin-10 regulates goblet cell numbers through Notch signaling in the developing zebrafish intestine, *Mucosal Immunol.* 15 (2022) 940–951, <https://doi.org/10.1038/s41385-022-00546-3>.
- [37] B.S. Mietto, A. Kroner, E.I. Girolami, E. Santos-Nogueira, J. Zhang, S. David, Role of IL-10 in resolution of inflammation and functional recovery after peripheral nerve injury, *J. Neurosci.* 35 (2015) 16431–16442, <https://doi.org/10.1523/JNEUROSCI.2119-15.2015>.
- [38] D.J. Hellenbrand, K.A. Reichl, B.J. Travis, M.E. Filipp, A.S. Khalil, D.J. Pulito, A.V. Gavigan, E.R. Maginot, M.T. Arnold, A.G. Adler, W.L. Murphy, A.S. Hanna, Sustained interleukin-10 delivery reduces inflammation and improves motor function after spinal cord injury, *J. Neuroinflammation* 16 (2019) 1–19, <https://doi.org/10.1186/s12974-019-1479-3>.
- [39] K. Ito, Y. Yoshiura, M. Ototake, T. Nakanishi, Macrophage migration inhibitory factor (MIF) is essential for development of zebrafish, *Danio rerio*, *Dev. Comp. Immunol.* 32 (2008) 664–672, <https://doi.org/10.1016/j.dci.2007.10.007>.
- [40] A. Honda, R. Abe, T. Makino, O. Norisugi, Y. Fujita, H. Watanabe, J. Nishihira, Y. Iwakura, S. ichi Yamagishi, H. Shimizu, T. Shimizu, Interleukin-1 β and macrophage migration inhibitory factor (MIF) in dermal fibroblasts mediate UVA-induced matrix metalloproteinase-1 expression, *J. Dermatol. Sci.* 49 (2008) 63–72, <https://doi.org/10.1016/j.jdermsci.2007.09.007>.
- [41] Y. Shen, D.L. Thompson, M.-K. Kuah, K.-L. Wong, K.L. Wu, S.A. Linn, E.M. Jewett, A.C. Shu-Chien, K.F. Barald, The cytokine macrophage migration inhibitory factor (MIF) acts as a neurotrophin in the developing inner ear of the zebrafish, *Danio rerio*, *Dev. Biol.* 363 (2012) 84–94, <https://doi.org/10.1016/j.ydbio.2011.12.023>.
- [42] R. Abe, T. Shimizu, A. Ohkawara, J. Nishihira, Enhancement of macrophage migration inhibitory factor (MIF) expression in injured epidermis and cultured fibroblasts, *Biochim. Biophys. Acta, Mol. Basis Dis.* 1500 (2000) 1–9, [https://doi.org/10.1016/S0925-4439\(99\)00080-0](https://doi.org/10.1016/S0925-4439(99)00080-0).
- [43] Y. Zhang, Y. Zhou, S. Chen, Y. Hu, Z. Zhu, Y. Wang, N. Du, T. Song, Y. Yang, A. Guo, Y. Wang, Macrophage migration inhibitory factor facilitates prostaglandin E2 production of astrocytes to tune inflammatory milieu following spinal cord injury, *J. Neuroinflammation* 16 (2019) 1–15, <https://doi.org/10.1186/s12974-019-1468-6>.
- [44] T.M. Tsarouchas, D. Wehner, L. Cavone, T. Munir, M. Keatinge, M. Lambertus, A. Underhill, T. Barrett, E. Kassapis, N. Ogryzko, Y. Feng, T.J. van Ham, T. Becker, C.G. Becker, Dynamic control of proinflammatory cytokines Il-1 β and Tnf- α by macrophages in zebrafish spinal cord regeneration, *Nat. Commun.* 9 (2018), <https://doi.org/10.1038/s41467-018-07036-w>.
- [45] M.A. Villarreal, N.M. Biediger, N.A. Bonner, J.N. Miller, S.K. Zepeda, B.J. Ricard, D.M. García, K.A. Lewis, Determining zebrafish epitope reactivity to commercially available antibodies, *Zebrafish* 14 (2017) 387–389, <https://doi.org/10.1089/zeb.2016.1401>.